**Advanced Geomatics**

http://publish.mersin.edu.tr/index.php/geomatics/index

***e-ISSN: 2791-8637***

# Time Series Analysis of Turkish National Sea Level Monitoring System (TUDES) Data for Amasra Station Example

**Ahsen Çelen*[1], Yasemin Şişman [1]**

[1]Ondokuz Mayıs University, Faculty of Engineering, Department of Geomatics Engineering, 55139, Samsun, Turkey; (21281032@stu.omu.edu.tr; ysisman@omu.edu.tr)

**Keywords**

Time series analysis,
Sea level,
TUDES,
Minitab.

**Research Article**

Received : 04.12.2023
Revised : 29.01.2024
Accepted : 29.01.2024
Published : 31.03.2024

* **Corresponding Author**
21281032@stu.omu.edu.tr

**Abstract**

The observation and prediction of sea level are crucial for various reasons including the vertical datum determination, crustal movement forecasting, oceanographic modeling, and coastal infrastructure planning. In Turkey, a sea level monitoring system has been established by the General Directorate of Mapping and aims to measure sea level. Through the Turkish National Sea Level Monitoring System (TUDES), sea level is monitored using data collected at 20 tide gauge stations at 15-minute intervals. Time series analysis is considered a highly suitable modeling and forecasting method for data that is periodically measured. In this study, time series analysis models including ARIMA, SARIMA, and Holt-Winter's methods were applied using data from the Amasra tide gauge station within the TUDES for the year 2019. Additionally, a prediction for January 2020 at the same station was performed. The results were compared with the measured tide gauge data to assess the performance of the models. Evaluation criteria included the Mean Absolute Percentage Error (MAPE) for the Holt-Winter's method and the corrected Akaike Information Criteria (AICc) for the ARIMA and SARIMA models. The SARIMA(3,0,0)(0,2,2) model with an AICc value of -1307.83, indicating a seasonality of 12, was observed to be the best-performing model.

## 1. Introduction

The main objectives of geodesy are to define the shape and size of the earth and to obtain data on the spatial information of points (Vanícek & Krakiwsky, 2015). Due to the inherent impracticality of directly performing mathematical calculations for the Earth's shape, various reference surfaces are employed to acquire positional information. Reference surfaces define the parameters necessary for the mathematical representation of geometric and physical quantities (Drewes, 2009). Depending on the scope and purpose of the study, different reference surfaces such as the sphere, ellipsoid, and geoid can be selected (Jekeli, 2016).

The geoid is an assumed equipotential still water surface that extends beneath the continents (Sansò & Sideris, 2013). This equilibrium surface used for vertical referencing can be determined through the long-term measurements of the average sea level. Sea level measurements observed over many years are reduced to the mean absolute sea level by removing various factors, in conjunction with geodetic measurements. The

**Cite this;**

*Çelen, A., & Şişman, Y. (2024). Time Series Analysis of Turkish National Sea Level Monitoring System (TUDES) Data for Amasra Station Example. Advanced Geomatics, 4(1), 37-47.*

reduced sea level is defined as the vertical datum (Altamimi et al., 2010). Therefore, the significance and analysis requirement of sea level measurements emerge.

The change of global mean sea level, as estimated from satellite data over the past few decades, is approximately +3mm per year (Cazenave et al., 2014). Nonetheless, this rate exhibits geographical non-uniformity and notable variations worldwide (Bindoff et al., 2007; Mitchum et al., 2010; Church et al., 2013).

Additionally, with the melting of land ice, the global mean sea level has risen by approximately 20 cm since the 1880s (Lindsey, 2022). This pronounced change in sea level not only plays a crucial role in determining vertical datum but is also of critical significance for regions around coastlines, particularly coastal areas. The future planning of coastal regions and the monitoring of environmental changes induced by global climate change, with appropriate actions taken accordingly, necessitate the continuous observation of sea levels.

Recent studies suggest that by the year 2100, sea levels could rise by 1 meter or more. This scenario poses a significant threat to coastal areas and ecosystems (Neumann et al., 2015).

Moreover, in the study utilizing sea level data observed between 2000 and 2018 and conducted by National Oceanic and Atmospheric Administration (NOAA), different scenarios were created based on future rates of greenhouse gas emissions, global warming, and variations in plausible rates of glacier and ice sheet loss. According to the 2022 report, even in the lowest greenhouse gas emission trajectory, it has been indicated that global mean sea levels are expected to rise by at least 0.3 meters by the year 2100. In a high-emission scenario triggering rapid ice sheet collapse, it has been highlighted that sea levels could rise up to 2 meters (Figure 1).

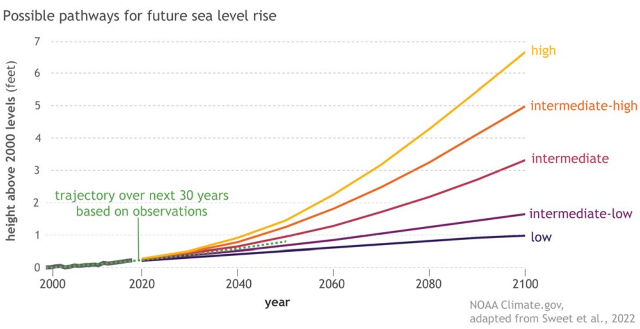


**Figure 1.** Possible pathways for future sea level rise.

As can be understood from the studies, the importance of observing sea level and taking appropriate actions is quite clear.

To obtain meaningful results from sea level changes, it is necessary to conduct long-term, intensive measurements. To this end, global collaboration is undertaken. The Intergovernmental Oceanographic Commission (IOC), a subsidiary of UNESCO, addresses this issue on a global scale and collaborates with organizations such as the World Meteorological Organization (WMO). The representation of Turkey within the IOC is carried out by the Turkish Naval Forces Office of Navigation, Hydrography and Oceanography (Turkish Naval Forces Office of Navigation, Hydrography and Oceanography, n.d.).

The need for the long-term monitoring of sea level changes with globally distributed tide gauge stations has led the IOC to establish the Global Sea Level Observing System (GLOSS) (Unesco, I., 1997). As of November 2023, the GLOSS system, comprising 290 tide gauge stations, covers a total of 90 countries (Global Sea Level Observing System, n.d.) (Figure 2). The coordinating institution for the system in Turkey is the General Directorate of Mapping (General Directorate of Mapping, n.d.).


**Figure 2.** Distribution of GLOSS system data points on the World map (Global Sea Level Observing System, n.d.).

The Permanent Service for Mean Sea Level (PSMSL), which provides data for most studies on the global sea level rise in the 20th century, is responsible for the collection, publication, analysis, and interpretation of sea level data. Established in 1933 with its headquarters in Liverpool, it operates under the umbrella of the National Oceanography Centre (NOC) (Permanent Service for Mean Sea Level, n.d.) (Figure 3).

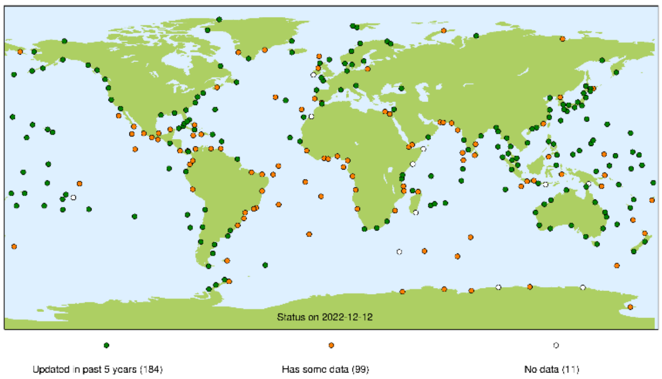


**Figure 3.** Distribution of PSMSL system data points on the World map (Permanent Service for Mean Sea Level, n.d.).

The Global Ocean Observing System (GOOS), another ocean observation system, is jointly supported by the IOC, WMO, and the United Nations Environment Programme (UNEP) (Global Ocean Observing System, n.d.). Operating under the umbrella of GOOS, the European Global Ocean Observing System (EuroGOOS) conducts its activities on a European scale. Established in Brussels in 1994, EuroGOOS is supported by national government institutions, research organizations, and private companies, boasting 44 members from 18 European countries (Figure 4) (European Global Ocean Observing System, n.d.).

EuroGOOS operates in five distinct regions: the Arctic (Arctic ROOS), the Baltic region (BOOS), the North West Shelf (NOOS), the Ireland-Biscay-Iberia region (IBI-ROOS), and the Mediterranean (MONGOOS) (European Global Ocean Observing System, n.d.).

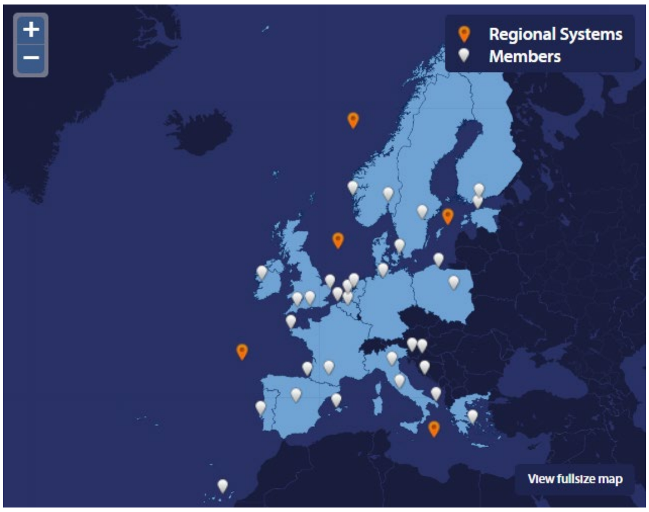


**Figure 4.** Map of EuroGOOS system member countries and regions (European Global Ocean Observing System, n.d.).

As mentioned above, the task of monitoring sea levels in Turkey is carried out by the General Directorate of Maps. Furthermore, under the umbrella of the General Directorate of Maps, the Turkey National Sea Level Monitoring System (TUDES) has been established for sea level observations (TUDES, n.d.) (Figure 5).

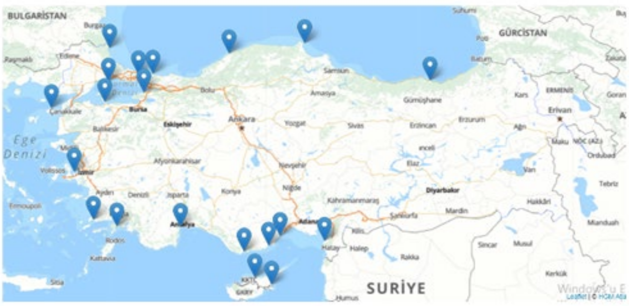


**Figure 5.** Distribution of TUDES system data points

If an organizational chart is prepared for institutions and organizations working towards the goal of sea level measurement worldwide, Figure 6 can be obtained:

To extract reliable information from data sets requiring long-term observations such as sea level, statistical analysis is necessary. Time series analysis, a type of statistical analysis, is a powerful option for examining sea level data. Time series analyses allow for understanding the stochastic mechanisms of the measured data and gaining insights into future predictions based on past data (Cryer & Chan, 2008).

Several exemplary studies exist that support the analysis of sea level data through time series, as mentioned in the paragraph above. For instance: a study predicting the surface water level of the Caspian Sea, which achieved successful results with the ARIMA model (Vaziri, 1997); a study emphasizing the sensitivity of low-lying island countries and using Exponential Smoothing and ARIMA models to forecast the sea level based on satellite altimeter data of the Arabian Sea, where the ARIMA model yielded better results (Srivastava et al., 2016); an analysis of the average sea level of Manila South Harbor using SARIMA models (Fernandez, 2018); a study integrating SARIMA and Long Short-Term Memory (LSTM) models for predicting sea level changes in the South China Sea, with a particular success in short-term sea level variations with centimeter-level precision (Sun et al., 2020); the prediction of tidal levels in Cilacap Bay using Holt-Winter's, ARIMA, and SARIMA methods (Wibowo et al., 2020); and a study forecasting the sea level along the West Peninsular Malaysia coastline using ARIMA, Support Vector Regression (SVR), and LSTM neural network models (Balogun et al., 2021) can be cited as examples.

In this study, the time series analysis in sea level data for the year 2019 at the Amasra tide gauge station was examined using time series analysis methods, including ARIMA, SARIMA, and Holt-Winter's, and forecasting were made for January 2020. The obtained forecast values were compared with the actual data, and the best model was observed to be SARIMA(3,0,0)(0,2,2) with an AICc value of -1307.83 and a seasonality of 12.

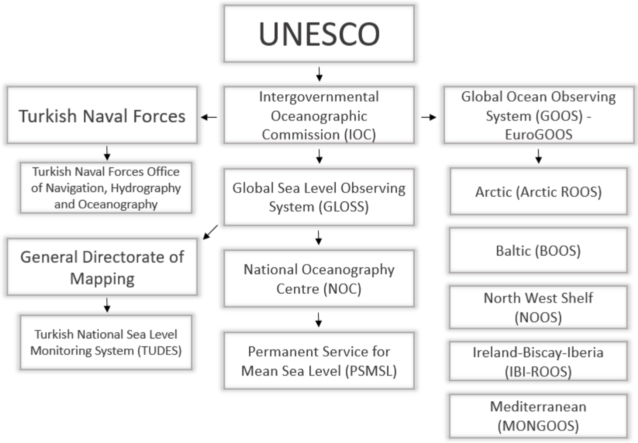


**Figure 6.** The organizational chart of institutions and organizations conducting sea level measurements.

## 2. Material and Methods

### 2.1. Material

The task of monitoring sea level in Turkey is conducted under the umbrella of the General Directorate of Mapping through the Turkish National Sea Level Monitoring System (TUDES) system, there are 20 GNSS-integrated radar sensor tide gauge stations distributed along the coasts of Turkey and the Turkish Republic of Northern Cyprus, adhering to GLOSS standards. These stations record measurements at 15-minute intervals, capturing not only sea level but also meteorological parameters affecting sea level changes, such as atmospheric pressure, wind speed, humidity, and temperature (TUDES, n.d.).

For the purposes of this study, TUDES data was provided by the General Directorate of Mapping, and the sea level data for the Amasra tide gauge station was accessed through the website https://tudes.harita.gov.tr/.


**Figure 7.** Study area.

In the year 2019, a total of 34,921 observation units were obtained for the Amasra tide gauge station. To organize and finalize this data, the following code snippet was written using the Python programming language, which calculates daily averages for each day:

```
import pandas as pd
df = pd.read_csv("C:/Users/PC/Desktop/Yüksek Lisans/TUDES veri/Ham veri/amasra'19.csv")
df['Tarih'] = pd.to_datetime(df['Tarih'])
df['Tarih'] = df['Tarih'].dt.date
daily_avg = df.groupby('Tarih')['Deger'].mean().reset_index()
daily_avg.to_csv("amasra19_daily_avg.csv", index=False)
print(daily_avg)

        Tarih     Deger
0   2019-01-01  0.489083
1   2019-01-02  0.475073
2   2019-01-03  0.507583
3   2019-01-04  0.489292
```

**Figure 8.** Code snippet to calculate daily averages.

The organized data was examined for general statistical information using the Minitab program, and tests for normality and outliers were conducted.

## 2.2. Method

Time series analysis examines the statistical distributions of periodic data within a specific time interval and consists of Autoregressive (AR) and Moving Average (MA) models.

In AR models, the dependent variable is considered as a function of its past values. In the AR(p) model, the $Y_t$ value is represented as a linear function of the weighted sum of the series' past p values and error terms, as shown in the equation:

$$Y_t = \mu + \phi_1 Y_{t-1} + \phi_2 Y_{t-2} + \ldots + \phi_p Y_{t-p} + \varepsilon_t$$

In this equation, $Y_{t-1}, Y_{t-2}, .., Y_{t-p}$ represent past observed values, μ represents the mean, $\varepsilon_t$ represents the error term, and $\phi_1, \phi_2, .., \phi_p$ represent the coefficients of past observations. The goal in the model is to obtain the model order that makes the sum of squared errors zero and determine the unknown coefficients (Kara, 2009).

In the MA method, the aim is to reduce the effects of momentary, erroneous, and outlier data on the overall data. There are various types of moving average (MA) methods, such as Simple, Cumulative, Weighted, and Exponential. The equation for the MA method is represented as:

$$Y_t = \mu + \varepsilon_t + \theta_1 \varepsilon_{t-1} + \ldots + \theta_q \varepsilon_{t-q}$$

Here, $\theta_1, \ldots, \theta_q$ represent the coefficients of error terms, μ represents the mean and $\varepsilon_t, \varepsilon_{t-1}, \ldots, \varepsilon_{t-q}$ represent the error terms. The right side of the equation is expressed in terms of a meaningful q number of errors. The error term in the equation has a mean of zero and a constant variance (Kara,2009).

### 2.3.1. Autoregressive Integrated Moving Average (ARIMA)

Many natural processes demonstrate inertia and do not undergo rapid changes. This characteristic, in conjunction with the sampling frequency, often leads to a correlation between successive observations. This sequential dependence is termed autocorrelation. When autocorrelation is present in the data, numerous standard modeling approaches, assuming independent observations, may become deceptive or, in some cases, entirely ineffective. Therefore, it is essential to explore alternative methodologies that consider the serial dependence inherent in the data. This can be relatively easily accomplished by utilizing time series models like Autoregressive Integrated Moving Average (ARIMA) models (Bisgaard & Kulahci, 2011).

ARIMA is a method used for performing univariate time series analysis and forecasting, also known as Box-Jenkins models. It represents an integrated model that incorporates operations such as MA, AR and differencing. In the model expressed as ARIMA(p, d, q), p denotes the degree of the autoregressive (AR) model, d represents the differencing operation, and q indicates the degree of the MA model (Cryer, 1986).

The fundamental objective of the Box-Jenkins forecasting method is to identify a suitable formula in order to minimize the residuals and ensure their absence of any discernible pattern (Afrifa-Yamoah et al., 2016).

The creation of the model occurs in three stages: identification, parameter determination, and prediction. In the identification stage, the stationarity of the series is examined. If the series is non-stationary, necessary processes such as differencing, autocorrelation or partial autocorrelation calculations are performed to make it stationary. In the parameter determination stage, decisions are made on the values of p, d, and q, and the choice of the ARIMA model. "p" represents how many past values are included in the regression for the current value, "d" indicates how many times differencing has been applied based on past data, and "q" represents how many past values are considered in the moving average. During this stage, ACF and PACF graphs of the stationary or stationarized series are examined, and a suitable model is selected accordingly. In the prediction stage, the accuracy value is calculated by examining the relationship between real and predicted values. Generally, the performance of the model is assessed using the mean squared error method (Erden, 2020).

The Box-Jenkins forecasting model is outlined in the diagram below (Afrifa-Yamoah et al., 2016) (Figure 9):

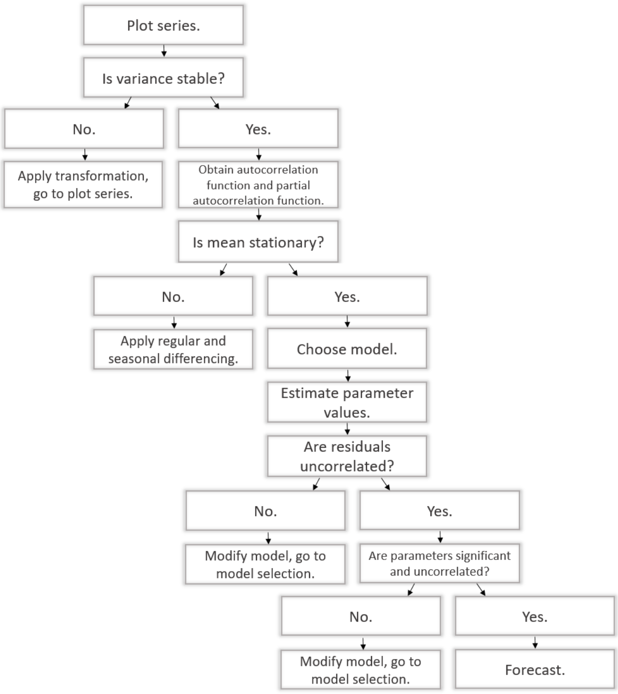


**Figure 9.** Box-Jenkins forecasting model diagram.

The ARIMA model is represented as shown below:

$$y_t = \alpha_0 + \sum_{t=1}^{p} \alpha_t (y_{t-1} - \mu) + \varepsilon_t$$

Here, $\alpha_0$ and $\alpha_t$ represent autoregressive parameters to be estimated, and $\varepsilon_t$ represents the random errors with zero mean and finite variances.

### 2.3.2. Seasonal Autoregressive Integrated Moving Average (SARIMA)

For time series data that exhibit seasonality and are non-stationary, ARIMA models often do not yield satisfactory results. Therefore, SARIMA models, which account for seasonality, are employed. In SARIMA models, denoted as SARIMA(p, d, q)(P, D, Q)$_s$, in addition to the parameters used in ARIMA (p, d, q), there are additional parameters P, D, and Q that represent the seasonal AR order, differencing operation, and seasonal MA order. Additionally, s represents the length of the season. These models take into consideration both the non-seasonal and seasonal components, offering a more comprehensive approach to time series modeling (Shumway & Stoffer, 2017).

If the ARIMA(*p, d, q*) model is represented as follows (Farhan and Ghim, 2018):

$$Y_t = \phi_1 Y_{t-1} + \phi_2 Y_{t-2} + \ldots + \phi_p Y_{t-p} + \varepsilon_t + \theta_1 \varepsilon_{t-1} + \ldots + \theta_q \varepsilon_{t-q}$$

$Y_{t-p}$ : time series data at different lags
$\phi$ and $\theta$ : unknown parameter
$p$ : AR order
$d$ : differencing order
$q$ : MA order
$\varepsilon$ : independently distributed term

The model can be shown more abbreviated:

$$\phi(L)\, \Delta^d\, y_t = \theta(L)\varepsilon_t$$

L : backshift or lag operator
$\Delta^d$ : difference $(1-L)^d$
$\phi$ and $\theta$ : lag operator polynomials

To include seasonal variation in the time series, the ARIMA model can be expanded in the following manner:

$$\Phi_P(L^s)\, \phi(L)\, \Delta_S^D \Delta^d\, y_t = \Theta_Q(L^S)\theta(L)\varepsilon_t$$

$\Delta_S^D$ : seasonal difference $(1-L)^D$
$\Theta$ and $\Phi$ : lag operator polynomials

### 2.3.3. Holt-Winter's

Exponential smoothing techniques are among the most commonly employed forecasting methods in various data sets (Gardner, 2006). Their popularity stems from their straightforward model formulation and their effectiveness in forecasting. Specifically, Holt-Winter's methods enable the handling of univariate time series that encompass both trend and seasonal factors (Bermúdez et al., 2010).

The Holt-Winters forecasting algorithm, developed by Charles Holt and Peter Winters, is employed to smooth time series data and utilize it for forecasting various aspects in the concerned data (Panda, 2020; Makatjane & Moroke, 2016). Exponential smoothing is a technique for smoothing time series data, assigning exponentially decreasing weights and values to past data. There are three types of exponential smoothing. The first type is single exponential smoothing for univariate time series forecasting. This type is utilized when the time series data lack a systematic structure, showing no trends and seasonality (Djauhari et al., 2020). This type of exponential smoothing utilizes a single parameter α, ranging between 0 and 1, as a smoothing factor. A smaller α value indicates slower learning, requiring more past observations for estimation, while a larger value indicates faster learning, relying on more recent observations for estimation (Panda, 2020).

The next type is double exponential smoothing, where, in addition to α, another smoothing parameter β is introduced for the change in trend. Two types of trends, additive trend providing linear trend analysis and multiplicative trend providing exponential trend analysis, are considered. During multi-step forecasts in the long term, it was observed that the trend is not a feasible possibility. Therefore, dampening may be practical by reducing the trend size for future forecasts with a straight line (Djakaria and Saleh, 2021).

Finally, the third type of exponential smoothing is the triple exponential smoothing method, a technique used when a series exhibits seasonal variations, allowing for seasonality. The triple exponential smoothing method depends on three parameters: α, β, and γ, with values ranging between zero and one, namely $0 < \alpha, \beta, \gamma$

< 1 (Shokeralla et al., 2020). The Holt-Winters triple exponential smoothing, named after its founders Charles Holt and Peter Winters, is the newest exponential smoothing method useful for identifying patterns of changing levels, trends, and seasons over time using additive or multiplicative seasons (Djakaria & Saleh, 2021).

The method involves a three-equation structure, accounting for level, trend, and seasonality. The seasonal equation can be formulated in two ways: multiplicative when trend and seasonality move together, and additive when they do not. (Hafid and Al-maamary, 2011). The model is represented as shown below:

Level:

$$L_t = \alpha\frac{Y_t}{S_{t-s}} + (1-\alpha)(L_{t-1} + m_{t-1})$$

Trend:

$$m_t = \beta(L_t - L_{t-1}) + (1-\beta)m_{t-1}$$

Seasonality:

$$S_t(t) = \gamma\frac{Y_t}{L_t} + (1-\gamma)\, S_{t-s}(t)$$

Forecast:

$$F_{t+\tau} = (L_t + m_t q)\, S_{t-s}(t)$$

Here; $\alpha$, $\beta$ and $\gamma$ are smoothing constants, t is the time period, $Y_t$ is the actual observed values, s is the length of seasonality, $L_t$ is the level component, $m_t$ is the trend component, $S_t$ is the seasonal component and $F_{t+\tau}$ is the forecast for $\tau$ periods ahead.

## 3. Application and Results

For all modeling, the 2021 version of the Minitab program was employed. The model evaluation criterion is based on corrected Akaike Information Criteria (AICc). AICc is essentially Akaike Information Criteria (AIC) with an extra penalty term for the number of parameters. The smaller AIC is, the better the model fits the data (Minitab, 2021).

The AIC is an information-theoretic indicator rooted in Kullback-Leibler Divergence, primarily assessing the information loss incurred by a given model. Consequently, the AIC criterion operates on the premise that the less information a model forfeits, the higher its quality (Kasali & Adeyemi, 2022).

On the other hand, the Bayesian Information Criterion (BIC) criteria are founded on Bayesian theory, with the goal of maximizing a model's posterior probability given the available data.The Bayesian Information Criterion serves as a pivotal tool in the realm of statistics for model selection from a finite set of options. It maintains a close relationship with the Akaike Information Criteria and is partly reliant on the likelihood function (Kasali & Adeyemi, 2022).

Here are the AICc and BIC formulas (Minitab, 2021):

$$AIC = 2[(\rho + 1) - L_c]$$

$$L_c(y_i\, \mu_i\, \Phi) = \sum_{i=1}^{n} l_i$$

$$l_i = \ln(f(y_i, \widehat{\mu_i}, \Phi))$$

$$y_i \ln(\widehat{\mu_i}) + (m_i - )\ln(1 - \widehat{\mu_i})$$

$p$: the regression degrees of freedom
$L_c$: the log-likelihood of the current model
$y_i$: the number of events for the $i^{th}$ row
$m_i$: the number of trials for the $i^{th}$ row
$\Phi$: 1, for binomial models
$\widehat{\mu_i}$: the estimated mean response of the $i$th row

$$AICc = -2\ln(\text{Likelihood}) + 2p + \frac{2p(p+1)}{n-p-1}$$

AICC is not calculated when $n - p - 1 \leq 0$

$$BIC = -2\ln(\text{Likelihood}) + p\ln(n)$$

Initially, the ARIMA model that does not account for seasonality was tested. The optimal parameters for the model were calculated with the assistance of the program, resulting in ARIMA(2,0,2) (Figure 10).

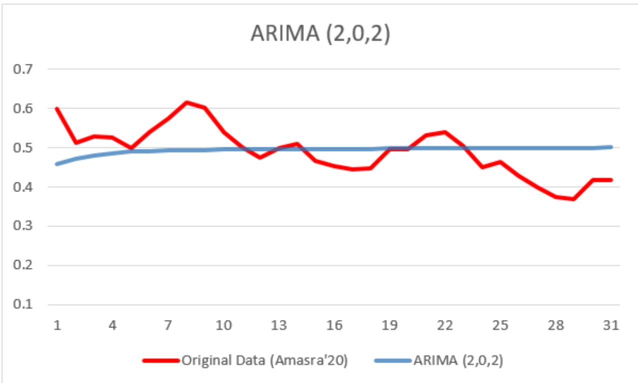


**Figure 10.** ARIMA(2,0,2) model.

Subsequently, in order to apply the SARIMA model that takes seasonality into account, all combinations of the following values were tested: "3, 4, 12" for seasonality, "0, 1, 2" for differencing, "0, 1, 2" for seasonal differencing (Figure 11a-11b-11c).

| | SARIMA | | | | | | | | |
|---|---|---|---|---|---|---|---|---|---|
| Seasonality | 12 | | | | | | | | |
| Difference | 0 | | | 1 | | | 2 | | |
| Seasonal Difference | 0 | 1 | 2 | 0 | 1 | 2 | 0 | 1 | 2 |
| | 0.465910 | 0.453857 | 0.455124 | 0.460844 | 0.457587 | 0.461052 | 0.456085 | 0.449090 | 0.44316 |
| | 0.479343 | 0.469606 | 0.466747 | 0.465717 | 0.476318 | 0.470528 | 0.464203 | 0.452957 | 0.41051 |
| | 0.492820 | 0.476546 | 0.486549 | 0.474713 | 0.482052 | 0.482416 | 0.468529 | 0.478646 | 0.38307 |
| | 0.496258 | 0.473416 | 0.482500 | 0.479874 | 0.477629 | 0.470380 | 0.470031 | 0.469965 | 0.33605 |
| | 0.493899 | 0.460243 | 0.467795 | 0.481914 | 0.465292 | 0.453021 | 0.467004 | 0.452229 | 0.28523 |
| | 0.495886 | 0.457365 | 0.482805 | 0.482313 | 0.461739 | 0.458700 | 0.468345 | 0.457309 | 0.26004 |
| | 0.512347 | 0.485956 | 0.562187 | 0.496179 | 0.488868 | 0.497876 | 0.480652 | 0.516988 | 0.32281 |
| | 0.510515 | 0.485376 | 0.543525 | 0.495109 | 0.489980 | 0.494781 | 0.478534 | 0.509906 | 0.27371 |
| | 0.515940 | 0.489359 | 0.538428 | 0.501507 | 0.493233 | 0.481807 | 0.481954 | 0.487753 | 0.24606 |
| | 0.510270 | 0.47782 | 0.495936 | 0.497958 | 0.482174 | 0.465035 | 0.476962 | 0.455546 | 0.16757 |
| | 0.511990 | 0.485531 | 0.500005 | 0.501090 | 0.491866 | 0.488646 | 0.477038 | 0.485425 | 0.15783 |
| | 0.499233 | 0.460074 | 0.452193 | 0.488562 | 0.466561 | 0.456199 | 0.467712 | 0.444263 | 0.04176 |
| | 0.500199 | 0.454442 | 0.449441 | 0.488013 | 0.461297 | 0.457822 | 0.467137 | 0.434011 | -0.01006 |
| | 0.502909 | 0.464140 | 0.456942 | 0.489267 | 0.472796 | 0.468210 | 0.467964 | 0.443836 | -0.06363 |
| | 0.505492 | 0.473307 | 0.478772 | 0.490601 | 0.482848 | 0.482242 | 0.468370 | 0.478553 | -0.10674 |
| | 0.505921 | 0.468269 | 0.476638 | 0.489955 | 0.477255 | 0.469431 | 0.468464 | 0.466415 | -0.18765 |
| | 0.506333 | 0.457118 | 0.462785 | 0.491429 | 0.467301 | 0.451907 | 0.468057 | 0.454785 | -0.26354 |
| | 0.506731 | 0.452048 | 0.480426 | 0.490466 | 0.462583 | 0.459370 | 0.468133 | 0.464107 | -0.31362 |
| | 0.507113 | 0.465782 | 0.567362 | 0.484792 | 0.473035 | 0.498866 | 0.469423 | 0.517541 | -0.29678 |
| | 0.507481 | 0.468182 | 0.546930 | 0.485897 | 0.475808 | 0.494516 | 0.469116 | 0.509181 | -0.37831 |
| | 0.507836 | 0.466909 | 0.542042 | 0.484576 | 0.473719 | 0.479466 | 0.469423 | 0.481148 | -0.45058 |
| | 0.508177 | 0.461227 | 0.495696 | 0.487058 | 0.469537 | 0.463412 | 0.468798 | 0.443305 | -0.55235 |
| | 0.508505 | 0.468650 | 0.499305 | 0.487340 | 0.476358 | 0.488099 | 0.468734 | 0.454587 | -0.59500 |
| | 0.508822 | 0.455572 | 0.447984 | 0.491295 | 0.466478 | 0.455981 | 0.467629 | 0.430646 | -0.71632 |
| | 0.509126 | 0.450725 | 0.445655 | 0.491174 | 0.461579 | 0.457870 | 0.467493 | 0.427267 | -0.79330 |
| | 0.509420 | 0.458767 | 0.453265 | 0.490974 | 0.469482 | 0.467914 | 0.467512 | 0.433330 | -0.87176 |
| | 0.509702 | 0.467964 | 0.476508 | 0.490508 | 0.478619 | 0.481807 | 0.467484 | 0.458512 | -0.93572 |
| | 0.509974 | 0.463380 | 0.474761 | 0.490041 | 0.474257 | 0.468457 | 0.467422 | 0.456588 | -1.03432 |
| | 0.510236 | 0.452419 | 0.461040 | 0.490061 | 0.463725 | 0.450380 | 0.467305 | 0.444796 | -1.13291 |
| | 0.510488 | 0.447446 | 0.480871 | 0.489873 | 0.459102 | 0.458149 | 0.467241 | 0.458105 | -1.20378 |
| | 0.510730 | 0.461301 | 0.574916 | 0.488167 | 0.473427 | 0.502982 | 0.467312 | 0.526798 | -1.19970 |

**Figure 11a.** SARIMA model combinations with seasonality 12.

| | SARIMA | | | | | | | | |
|---|---|---|---|---|---|---|---|---|---|
| Seasonality | 4 | | | | | | | | |
| Difference | 0 | | | 1 | | | 2 | | |
| Seasonal Difference | 0 | 1 | 2 | 0 | 1 | 2 | 0 | 1 | 2 |
| | 0.468887 | 0.452040 | 0.484054 | 0.47108 | 0.468362 | 0.456437 | 0.464689 | 0.436706 | 0.42262 |
| | 0.483204 | 0.455681 | 0.468872 | 0.48322 | 0.483028 | 0.442939 | 0.469755 | 0.412461 | 0.32769 |
| | 0.475302 | 0.469337 | 0.490775 | 0.48423 | 0.490503 | 0.471341 | 0.481632 | 0.403113 | 0.28532 |
| | 0.476880 | 0.454376 | 0.452009 | 0.48547 | 0.480254 | 0.442696 | 0.474204 | 0.363764 | 0.15712 |
| | 0.472184 | 0.438723 | 0.468464 | 0.47992 | 0.464287 | 0.434901 | 0.477904 | 0.334055 | 0.07115 |
| | 0.479914 | 0.443102 | 0.466248 | 0.48747 | 0.471272 | 0.426239 | 0.472360 | 0.308523 | -0.07196 |
| | 0.499442 | 0.471470 | 0.506780 | 0.50017 | 0.487817 | 0.464818 | 0.475465 | 0.295004 | -0.16054 |
| | 0.506444 | 0.466937 | 0.480535 | 0.50819 | 0.492158 | 0.443222 | 0.471535 | 0.260069 | -0.33780 |
| | 0.513748 | 0.457964 | 0.491689 | 0.51035 | 0.483923 | 0.438493 | 0.473191 | 0.228307 | -0.47142 |
| | 0.505677 | 0.454854 | 0.479232 | 0.50402 | 0.481546 | 0.424877 | 0.470327 | 0.201496 | -0.66384 |
| | 0.507603 | 0.479218 | 0.511150 | 0.50455 | 0.493664 | 0.456747 | 0.471236 | 0.186125 | -0.80043 |
| | 0.492698 | 0.465285 | 0.478317 | 0.49502 | 0.487121 | 0.427899 | 0.469041 | 0.152235 | -1.02813 |
| | 0.494215 | 0.456186 | 0.487911 | 0.49699 | 0.481583 | 0.420750 | 0.469381 | 0.119433 | -1.21065 |
| | 0.498545 | 0.454166 | 0.475379 | 0.49722 | 0.481823 | 0.410241 | 0.467630 | 0.091589 | -1.45378 |
| | 0.499674 | 0.478620 | 0.509446 | 0.49580 | 0.494932 | 0.449304 | 0.467601 | 0.075117 | -1.63978 |
| | 0.500733 | 0.464571 | 0.477220 | 0.49459 | 0.487449 | 0.424978 | 0.466158 | 0.041122 | -1.91929 |
| | 0.501725 | 0.455457 | 0.488371 | 0.49375 | 0.481373 | 0.419926 | 0.465877 | 0.007539 | -2.15208 |
| | 0.502656 | 0.453454 | 0.475843 | 0.49540 | 0.481667 | 0.405888 | 0.464641 | -0.021171 | -2.44730 |
| | 0.503529 | 0.477914 | 0.510649 | 0.49675 | 0.495017 | 0.440698 | 0.464190 | -0.038496 | -2.68409 |
| | 0.504347 | 0.463866 | 0.477371 | 0.49879 | 0.487592 | 0.411201 | 0.463094 | -0.072993 | -3.01679 |
| | 0.505115 | 0.454754 | 0.488856 | 0.49876 | 0.481460 | 0.404527 | 0.462528 | -0.107299 | -3.30122 |
| | 0.505834 | 0.452753 | 0.475734 | 0.49805 | 0.481710 | 0.392423 | 0.461526 | -0.136791 | -3.64990 |
| | 0.506509 | 0.477215 | 0.511182 | 0.49833 | 0.495063 | 0.432404 | 0.460882 | -0.154882 | -3.93885 |
| | 0.507142 | 0.463169 | 0.477029 | 0.49745 | 0.487656 | 0.405715 | 0.459945 | -0.19002 | -4.32612 |
| | 0.507735 | 0.454059 | 0.489102 | 0.49777 | 0.481529 | 0.400480 | 0.459248 | -0.22504 | -4.66357 |
| | 0.508291 | 0.452059 | 0.475587 | 0.49756 | 0.481774 | 0.385814 | 0.458354 | -0.255276 | -5.06708 |
| | 0.508813 | 0.476522 | 0.511787 | 0.49724 | 0.495125 | 0.423206 | 0.457622 | -0.274103 | -5.40958 |
| | 0.509302 | 0.462477 | 0.476790 | 0.49681 | 0.487717 | 0.392757 | 0.456756 | -0.309931 | -5.85279 |
| | 0.509760 | 0.453368 | 0.489428 | 0.49672 | 0.481591 | 0.386441 | 0.456001 | -0.345665 | -6.24463 |
| | 0.510191 | 0.451369 | 0.475484 | 0.49699 | 0.481837 | 0.372913 | 0.455155 | -0.376629 | -6.70436 |
| | 0.510594 | 0.475832 | 0.512404 | 0.49709 | 0.495187 | 0.414106 | 0.454383 | -0.39618 | -7.10177 |

**Figure 11b.** SARIMA model combinations with seasonality 4.

| | SARIMA | | | | | | | | |
|---|---|---|---|---|---|---|---|---|---|
| **Seasonality** | 3 | | | | | | | | |
| **Difference** | 0 | | | 1 | | | 2 | | |
| **Seasonal Difference** | 0 | 1 | 2 | 0 | 1 | 2 | 0 | 1 | 2 |
| | 0.459586 | 0.457555 | 0.487911 | 0.461314 | 0.470043 | 0.489928 | 0.458477 | 0.438783 | 0.388540 |
| | 0.479844 | 0.473319 | 0.478968 | 0.472513 | 0.487182 | 0.478748 | 0.472099 | 0.409950 | 0.255600 |
| | 0.491059 | 0.479280 | 0.467067 | 0.482181 | 0.494194 | 0.467646 | 0.470284 | 0.379367 | 0.146020 |
| | 0.493117 | 0.482886 | 0.493915 | 0.482355 | 0.490831 | 0.471044 | 0.467984 | 0.334889 | 0.022850 |
| | 0.491284 | 0.488355 | 0.484765 | 0.485398 | 0.489144 | 0.461656 | 0.468271 | 0.304007 | -0.10591 |
| | 0.497150 | 0.487637 | 0.469071 | 0.488023 | 0.485759 | 0.439720 | 0.468287 | 0.268571 | -0.26442 |
| | 0.497606 | 0.487855 | 0.513048 | 0.488060 | 0.487982 | 0.467042 | 0.467917 | 0.233891 | -0.41077 |
| | 0.497010 | 0.491414 | 0.505356 | 0.488878 | 0.490841 | 0.455587 | 0.467643 | 0.197843 | -0.60970 |
| | 0.497549 | 0.489521 | 0.488087 | 0.489583 | 0.487831 | 0.442643 | 0.467420 | 0.160151 | -0.78751 |
| | 0.498072 | 0.489009 | 0.495620 | 0.489581 | 0.488388 | 0.449157 | 0.467173 | 0.124869 | -0.98016 |
| | 0.498579 | 0.492118 | 0.493227 | 0.489793 | 0.490553 | 0.439100 | 0.466922 | 0.090265 | -1.18762 |
| | 0.499071 | 0.489950 | 0.449088 | 0.489974 | 0.487814 | 0.417347 | 0.466675 | 0.050779 | -1.42161 |
| | 0.499548 | 0.489269 | 0.478610 | 0.489962 | 0.488736 | 0.443217 | 0.466429 | 0.014235 | -1.64230 |
| | 0.500010 | 0.492275 | 0.473945 | 0.490009 | 0.490943 | 0.431447 | 0.466182 | -0.020847 | -1.91130 |
| | 0.500458 | 0.490043 | 0.448552 | 0.490047 | 0.488096 | 0.416869 | 0.465934 | -0.060602 | -2.16359 |
| | 0.500893 | 0.489324 | 0.477150 | 0.490032 | 0.48896 | 0.426032 | 0.465687 | -0.098164 | -2.43148 |
| | 0.501314 | 0.492305 | 0.473532 | 0.490034 | 0.491182 | 0.415342 | 0.465440 | -0.134122 | -2.71992 |
| | 0.501723 | 0.490059 | 0.443776 | 0.490033 | 0.488361 | 0.393587 | 0.465193 | -0.174501 | -3.03064 |
| | 0.502119 | 0.489330 | 0.475897 | 0.490017 | 0.48923 | 0.418424 | 0.464946 | -0.212696 | -3.32793 |
| | 0.502503 | 0.492306 | 0.473563 | 0.490006 | 0.491445 | 0.406306 | 0.464698 | -0.249467 | -3.67208 |
| | 0.502876 | 0.490057 | 0.441269 | 0.489995 | 0.48862 | 0.390260 | 0.464451 | -0.290613 | -4.00407 |
| | 0.503237 | 0.489326 | 0.465606 | 0.489979 | 0.489489 | 0.401696 | 0.464204 | -0.329503 | -4.35123 |
| | 0.503587 | 0.492301 | 0.465173 | 0.489965 | 0.491706 | 0.390402 | 0.463957 | -0.366986 | -4.72258 |
| | 0.503927 | 0.490051 | 0.425763 | 0.489951 | 0.488881 | 0.368495 | 0.463710 | -0.408886 | -5.11240 |
| | 0.504256 | 0.489320 | 0.456952 | 0.489935 | 0.489750 | 0.392637 | 0.463463 | -0.448516 | -5.48980 |
| | 0.504575 | 0.492294 | 0.456622 | 0.489920 | 0.491967 | 0.380145 | 0.463215 | -0.486720 | -5.91406 |
| | 0.504884 | 0.490044 | 0.420885 | 0.489905 | 0.489142 | 0.362766 | 0.462968 | -0.529348 | -6.32994 |
| | 0.505184 | 0.489313 | 0.451986 | 0.489889 | 0.490011 | 0.376172 | 0.462721 | -0.569716 | -6.75961 |
| | 0.505475 | 0.492287 | 0.452769 | 0.489874 | 0.492228 | 0.364298 | 0.462474 | -0.608653 | -7.21616 |
| | 0.505757 | 0.490037 | 0.413992 | 0.489858 | 0.489403 | 0.342119 | 0.462227 | -0.652010 | -7.68834 |
| | 0.506031 | 0.489305 | 0.446336 | 0.489843 | 0.490272 | 0.365837 | 0.461980 | -0.693110 | -8.14978 |

**Figure 11c.** SARIMA model combinations with seasonality 3.

According to the AICc criterion, the models that provided the best results were:

SARIMA models with seasonality 3 of SARIMA(0,1,0)(1,2,3) and SARIMA(0,0,2)(3,2,0) (Figure 12a):

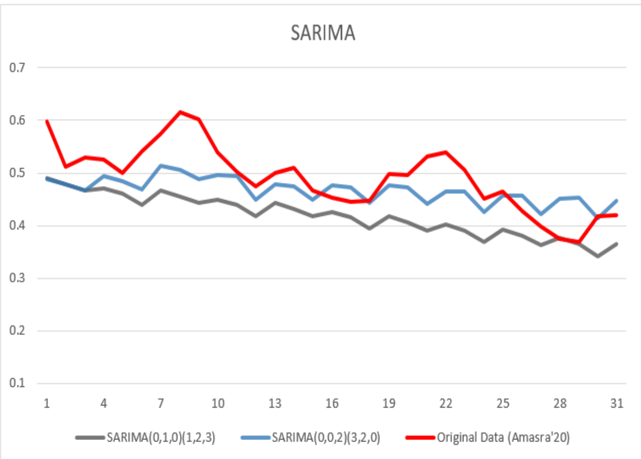


**Figure 12a.** SARIMA(0,1,0) (1,2,3) and SARIMA(0,0,2) (3,2,0) models.

SARIMA models with seasonality 4 of SARIMA(0,1,0)(1,2,3)(Figure 12b):

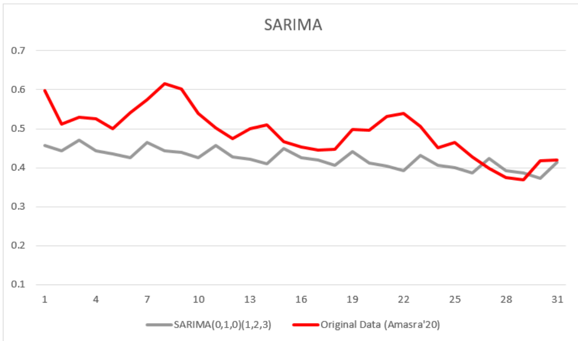


**Figure 12b.** SARIMA(0,1,0)(1,2,3) model.

SARIMA models with seasonality 12 of SARIMA(3,0,0)(0,2,2) and SARIMA(1,2,2)(3,1,0) (Figure 12c):

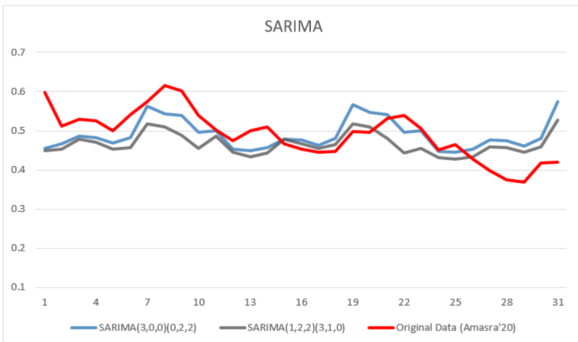


**Figure 12c.** SARIMA(3,0,0)(0,2,2) and SARIMA(1,2,2)(3,1,0) models.

The model performance summaries of ARIMA and SARIMA models were made according to Mean Square Error (MSD), AICc and BIC values (Table 1):

**Table 1.** Model Summaries.

| Model | MSD | AICc (-) | BIC (-) |
|---|---|---|---|
| ARIMA(2,0,2) | 0.0007982 | 1553.29 | 1530.13 |
| SARIMA(0,1,0)(1,2,3)$_3$ | 0.0010915 | 1389.50 | 1370.26 |
| SARIMA(0,0,2)(3,2,0)$_3$ | 0.0010598 | 1407.44 | 1384.37 |
| SARIMA(0,1,0)(1,2,3)$_4$ | 0.0009654 | 1420.31 | 1401.10 |
| SARIMA(3,0,0)(0,2,2)$_{12}$ | 0.0010689 | 1307.83 | 1285.09 |
| SARIMA(1,2,2)(3,1,0)$_{12}$ | 0.0010199 | 1365.45 | 1338.75 |

Here what the abbreviations represent:

MSD: Mean Square Deviation
AICc: Corrected Akaike Information Criteria
BIC: Bayesian Information Criterion

Finally, the Holt-Winter's method was applied to the data. Sequentially, combinations of α, β, and γ parameters ranging from "0.1 to 0.9" were tested for seasonality values of "3, 4, and 12". The best result was obtained with a seasonality of "4" and α, β, γ parameters set to "0.4", which was adopted in the additive model (Figure 13).

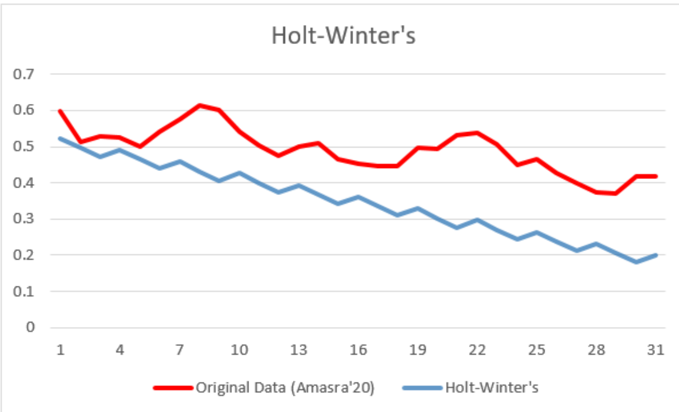


**Figure 13.** Holt-Winter's model.

The obtained outputs to evaluate the model are as follows:

**Table 1.** Holt-Winter's model accuracy measures.

| Measures | MAPE | MAD | MSD |
|---|---|---|---|
| Values | 6.29203 | 0.03136 | 0.00161 |

Here what the abbreviations represent:

MSD: Mean Square Deviation
MAD: Mean Absolute Deviation
MAPE: Mean Absolute Percent Error

MSD formula:

$$\frac{\sum_{t=1}^{n} |y_t - \hat{y_t}|^2}{n}$$

MAD formula:

$$\frac{\sum_{t=1}^{n} |y_t - \hat{y_t}|}{n}$$

MAPE formula:

$$\frac{\sum |y_t - \hat{y_t}| \,/\, y_t}{n} \; x \; 100 \; (y_t \neq 0)$$

Notation:

$y_t$ : actual value at time t
$\hat{y_t}$ : fitted value
$n$ : number of observations

## 4. Conclusion

In the scope of this study, time series analysis models, including ARIMA, SARIMA, and Holt-Winter's methods, were applied using the 2019 data from the Amasra tide gauge station within the TUDES system. Furthermore, forecasting were made for the same station for the month of January 2020. The obtained results were compared with the measured tide gauge data, and the model's performance was assessed. Evaluation criteria included the MSD for the Holt-Winter's method and the AICc for the ARIMA and SARIMA models. The best model observed was the SARIMA(3,0,0)(0,2,2) model with an AICc value of "-1307.83", indicating a seasonality of "12". And finally, the MSD value of SARIMA(3,0,0)(0,2,2)$_{12}$ method was compared with the MSD value of the Holt Winter's method, revealing that the SARIMA model with the value of " 0.0010689" outperformed the Holt-Winter's method with the value of "0.00161".

At the light of these explanation and applications it is said that the SARIMA(3,0,0)(0,2,2)$_{12}$ model is more suitable for these sea level data.

## Acknowledgments

The authors thank the General Directorate of Mapping for providing the sea level data.

## Author contributions

The contributions of the authors to the article should be stated.

## Conflicts of interest

There is no conflict of interest between the authors.

## Statement of Research and Publication Ethics

Research and publication ethics were complied with in the study.

## References

Afrifa-Yamoah, E., Saeed, B. I., & Karim, A. (2016). Sarima modelling and forecasting of monthly rainfall in the

Brong Ahafo Region of Ghana. *World Environment*, *6*(1), 1-9.

Al-Hafid, M. S., & Hussein Al-maamary, G. (2012). Short term electrical load forecasting using holt-winters method. *Al-Rafidain Engineering Journal (AREJ)*, *20*(6), 15-22.

Balogun, A. L., & Adebisi, N. (2021). Sea level prediction using ARIMA, SVR and LSTM neural network: assessing the impact of ensemble Ocean-Atmospheric processes on models' accuracy. *Geomatics, Natural Hazards and Risk*, *12*(1), 653-674.

Bermúdez, J. D., Segura, J. V., & Vercher, E. (2010). Bayesian forecasting with the Holt–Winters model. *Journal of the Operational Research Society*, *61*(1), 164-171.

Bisgaard, S., & Kulahci, M. (2011). *Time series analysis and forecasting by example*. John Wiley & Sons.

Blewitt, G., Altamimi, Z., Davis, J., Gross, R., Kuo, C. Y., Lemoine, F. G., ... & Zerbini, S. (2010). Geodetic observations and global reference frame contributions to understanding sea-level rise and variability. *Understanding sea-level rise and variability*, 256-284.

Cryer, J. D., Chan, K. S., & Kung-Sik.. Chan. (2008). *Time series analysis: with applications in R* (Vol. 2). New York: Springer. doi: 10.1007/978-0-387-75959-3

Cryer, J. D. (1986). *Time Series Analysis*. Retrieved from https://books.google.com.tr/books ?id=HVUZAQAAIAAJ

Djakaria, I., & Saleh, S. E. (2021, May). Covid-19 forecast using Holt-Winters exponential smoothing. In *Journal of physics: conference series* (Vol. 1882, No. 1, p. 012033). IOP Publishing.

Djauhari, M. A., Asrah, N. M., Li, L. S., Djakaria, I., Badruzzaman, S. T. A. I. K., & KM10, J. R. S. (2020). Forecasting model of electricity consumption in malaysia: A geometric Brownian motion approach. *Solid State Technology*, *63*(3), 40-46.

Drewes, H. (2009). Reference systems, reference frames, and the geodetic datum. In *Observing our changing Earth* (pp. 3-9). Springer Berlin Heidelberg.

Wibowo, D. S., Adytia, D., & Saepudin, D. (2020, August). Prediction of tide level by using holtz-winters exponential smoothing: Case study in cilacap bay. In *2020 International Conference on Data Science and Its Applications (ICoDSA)* (pp. 1-5). IEEE.

Erden, C. (2020). *Zaman serisi analizleri.* [PDF document]. Lecture Notes.

European Global Ocean Observing System. (n.d.). *Overview*. UNESCO.

Farhan, J., & Ong, G. P. (2018). Forecasting seasonal container throughput at international ports using SARIMA models. *Maritime Economics & Logistics*, *20*, 131-148.

Fernandez, F. R. Q., Montero, N. B., Po III, R. B., Addawe, R. C., & Diza, H. M. R. (2018). Forecasting Manila South Harbor Mean Sea Level Using Seasonal ARIMA Models. *Journal of Technology Management and Business*, *5*(1).

Gardner Jr, E. S. (2006). Exponential smoothing: The state of the art—Part II. *International journal of forecasting*, *22*(4), 637-666.

Global Ocean Observing System. (n.d.). *Who we are.* UNESCO.
https://www.goosocean.org/

Global Sea Level Observing System (n.d.). UNESCO.
https://gloss-sealevel.org/

Jekeli, C. (2016). Geometric Reference Systems in Geodesy (2016 edition).

Kara, T. (2009). *Sabit GPS istasyonlarında zaman serileri analizi* (Master's thesis, Fen Bilimleri Enstitüsü).

Lindsey R. (2022, 19 Nisan). *Climate change: global sea level.* National Oceanic and Atmospheric Administration. https://www.climate.gov/news-features/understanding-climate/climate-change-global-sea-level

Makatjane, K., & Moroke, N. (2016). Comparative study of holt-winters triple exponential smoothing and seasonal Arima: forecasting short term seasonal car sales in South Africa. *Makatjane KD, Moroke ND*.

Minitab, LLC. (2021). *Minitab*. Retrieved from https://support.minitab.com/en-us/minitab/21/ help-and-how-to/statistical- modeling/doe/how-to/factorial/analyze-binary-response/methods-and-formulas/model-summary/

Manual, F. P. (2010). National Oceanic and Atmospheric Administration. *Office of Coast Survey*, 154-155. https://www.noaa.gov/

Neumann, B., Vafeidis, A. T., Zimmermann, J., & Nicholls, R. J. (2015). Future coastal population growth and exposure to sea-level rise and coastal flooding-a global assessment. *PloS one*, *10*(3), e0118571.

Panda, M. (2020). Application of ARIMA and Holt-Winters forecasting model to predict the spreading of COVID-19 for India and its states. *medRxiv*, 2020-07.

Permanent Service for Mean Sea Level. (n.d.). National Oceanography Centre. Turkish Naval Forces Office of Navigation, Hydrography and Oceanography. (n.d.).
https://www.shodb.gov.tr/

Sansò, F., & Sideris, M. G. (Eds.). (2013). *Geoid determination: theory and methods*. Springer Science & Business Media.

Bezerra, A. K. L., & Santos, É. M. C. (2020). Prediction the daily number of confirmed cases of COVID-19 in Sudan with ARIMA and Holt Winter exponential smoothing. *International Journal of Development Research*, *10*(08), 39408-39413.

Shumway, R. H., Stoffer, D. S., & Stoffer, D. S. (2000). *Time series analysis and its applications* (Vol. 3). New York: springer.

Srivastava, P. K., Islam, T., Singh, S. K., Petropoulos, G. P., Gupta, M., & Dai, Q. (2016). Forecasting Arabian Sea level rise using exponential smoothing state space models and ARIMA from TOPEX and Jason satellite radar altimeter data. *Meteorological applications*, *23*(4), 633-639.

Sun, Q., Wan, J., & Liu, S. (2020). Estimation of sea level variability in the China Sea and its vicinity using the SARIMA and LSTM models. *IEEE Journal of Selected Topics in Applied Earth Observations and Remote Sensing*, *13*, 3317-3326.

Sweet, W. V., Kopp, R. E., Weaver, C. P., Obeysekera, J., Horton, R. M., Thieler, E. R., & Zervas, C.

(2017). *Global and regional sea level rise scenarios for the United States* (No. CO-OPS 083).

Torge, W., Müller, J., & Pail, R. (2023). *Geodesy*. Retrieved from https://books.google.com.tr/books?id=_4q0EAAAQBAJ

Türkiye Ulusal Deniz Seviyesi İzleme Sistemi. (t.y.). *Deniz seviyesi gözlemleri.* Harita Genel Müdürlüğü. https://tudes.harita.gov.tr/Portal/Index/32?lang=tr/Deniz%20Seviyesi%20G%C3%Gözlemleri.

Vanícek, P., Krakiwsky, E.J. (2015). *Geodesy: The concepts (Revised 2. Edition).* North-Holland, Amsterdam. Elsevier.

Vaziri, M. (1997). Predicting Caspian Sea surface water level by ANN and ARIMA models. *Journal of waterway, port, coastal, and ocean engineering*, *123*(4), 158-162.